Stark broadening in hot, dense laser-produced plasmas*

Richard J. Tighe and C. F. Hooper, Jr.
Physics Department, University of Florida, Gainesville, Florida 32611
(Received 26 April 1976)

Broadened Lyman-α x-ray lines from neon x and argon xviii radiators, which are immersed in a hot, dense deuterium or deuterium-tritium plasma, are discussed. In particular, these lines are analyzed for several temperature-density cases, characteristic of laser-produced plasmas; special attention is paid to the relative importance of ion, electron, and Doppler effects.

I. INTRODUCTION

With the availability of high-powered lasers, it is now possible to produce extremely hot plasmas that are also very dense. Such laser-produced plasmas are currently being studied intensively both in the United States and abroad. An integral part of these investigations is the development of diagnostics for the resulting plasmas. One proposed diagnostic technique would employ x-ray line broadening to determine plasma densities.[1] Experiments on laser-produced plasmas of moderate densities seem to confirm that Stark broadening may be utilized as a diagnostic for high-density laser-produced plasmas.[2,3] Recently Yaakobi and Goldman[4] and Burkhalter[5] reported the observation of Stark-broadened x-ray lines originating in these dense, hot laser-produced plasmas.

Some of the experiments being conducted at the Lawrence Livermore Laboratory involve the laser-induced implosion of glass-encapsulated deuterium-tritium gas targets. It has been proposed that these gas targets be seeded with a small amount of higher-Z impurity, such as neon or argon.[6] Then, for the expected temperature-density conditions produced by the implosion, the D-T plasma would be fully ionized and the impurity would be chosen so that the ion would be hydrogenic. Calculations indicate that some of the Lyman-series members of Ar XVIII, and possibly also of Ne X, will have sufficient intensity to be observed.

In this paper we consider the situation in which a D or D-T gas, seeded with a small percentage of neon or argon, is brought to conditions of temperature and density sufficient to strip a large fraction of the impurity atoms of all but one electron. Under these conditions it should be possible to observe the Lyman series of x rays. Hence we will consider Lyman-α radiation from Ne X and/or Ar XVIII radiators that are immersed in a fully ionized D or D-T plasma. Our purpose here in studying the broadening of the Lyman-α line for both hydrogenic neon and argon is to illustrate how such x-ray lines will be broadened under these extreme conditions. We will analyze these Lyman-α lines for various temperature-density cases, paying special attention to the relative importance to the broadening from ion, electron, and Doppler effects. We will then compare our results to those previously found for neutral hydrogen and ionized helium radiators immersed in more conventional plasmas.

In Sec. II we discuss the theoretical formalism; in Sec. II A we treat the problem of calculating the appropriate electric microfield distribution at a radiator of charge χe. Also in Sec. II, especially in Sec. II B, we discuss the formalism necessary to combine the static electric microfield contributions with those due to electron and Doppler broadening. In Sec. III we discuss our results, and in Sec. IV we present our conclusions together with comments regarding future work.

II. FORMALISM

The calculations performed herein are based on a formalism developed in Refs. 7 and 8. In this section we sketch this development, as modified for the case of a hydrogenic, high-Z radiator immersed in a D-T plasma. Following this, we comment on the range of validity of this theory.

For an ion undergoing spontaneous electric dipole transitions in the presence of a plasma, the intensity distribution of the emitted radiation is given by[9]

$$I(\omega) = \int_0^\infty P(\mathcal{E}) J(\omega, \mathcal{E})\, d\mathcal{E}\,. \tag{1}$$

In this expression, which uses the quasistatic approximation for the ions, $P(\mathcal{E})$ is the probability distribution function for the electric microfield due to the static ions. An equilibrium average over the ions is now contained in the microfield integration of Eq. (1). $J(\omega, \mathcal{E})$ contains the trace over the internal states of the radiating ion as well as the average over the perturbing electrons[8,9]:

$$J(\omega,\mathcal{E}) = -\pi^{-1}\,\mathrm{Im}\,\mathrm{Tr}_R\{\vec{d}\cdot[\Delta\omega - e\vec{\mathcal{E}}\cdot\vec{R}/\hbar - \mathcal{K}(\omega)]^{-1}(\rho^{(R)}\vec{d})\}\ ; \tag{2}$$

$\vec{d}$ is the dipole moment operator for the radiating ion and $\Delta\omega$ is the frequency separation from the transition in absence of the plasma. The second term inside the square brackets contains the ion-broadening effects; $\vec{R}$ is the position operator for the bound radiator electron. Averaged electron-broadening effects appear in the term $\mathcal{K}(\omega)$.

A final step in the calculation involves the inclusion of Doppler broadening by a convolution of the Stark profile with a Doppler profile.[10]

A. Electric microfield calculation

The calculation of $P(\mathcal{E})$ involves the evaluation of the following sine transform:[7,11]

$$P(\mathcal{E}) = 2\pi^{-1}\mathcal{E}\int_0^\infty T(L)\sin(\mathcal{E}L)L\,dL\ , \tag{3}$$

where

$$T(L) = \exp[-\gamma L^2 + I_1(L) + I_2(L)]\ . \tag{4}$$

γ, $I_1(L)$, and $I_2(L)$ have been calculated by a collective coordinate method.[7,11] The results are

$$\gamma = [a/4(\alpha^2-2)][\alpha^5 + 2(1-2\sqrt{2})\alpha^4 + 3\alpha^3 + 8(\sqrt{2}-1)\alpha^2 - 6\alpha + 4(2-\sqrt{2})]\ , \tag{5}$$

$$I_1(L) = 3\int dx\, x^2 e^{S(x)}\left[e^{-\beta w_{10}(x)}\left(\frac{\sin[LG(x)]}{LG(x)} - 1\right) - \left(\frac{\sin[Lq(x)]}{Lq(x)} - 1\right)\right], \tag{6}$$

where

$$\beta w_{10}(x) = \chi(a^2/3x)e^{-\alpha a x}\ , \tag{7}$$

$$S(x) = \chi(a^2/3x)[(\alpha^2-1)/(\alpha^2-2)](e^{-\alpha a x} - e^{-\sqrt{2}\alpha x})\ , \tag{8}$$

$$q(x) = -\left(\frac{\alpha^2-1}{\alpha^2-2}\right)\left(\frac{1}{x^2}(e^{-\alpha a x} - e^{-\sqrt{2}\alpha x}) + \frac{a}{x}(\alpha e^{-\alpha a x} - \sqrt{2}e^{-\sqrt{2}\alpha x})\right), \tag{9}$$

$$G(x) = q(x) + (1/x^2)e^{-\alpha a x}(1+\alpha a x)\ . \tag{10}$$

α is an effective range parameter, the choice of which is well discussed in Refs. 11 and 12. We note here that $P(\mathcal{E})$ is essentially parametrized by the two constants a and χ:

$$\begin{aligned} I_2(L) &= 3a^2\sum_k (-1)^k(2k+1)\mathfrak{a}\ , \\ \mathfrak{a} &= \int_0^\infty x_2^{3/2} I_{k+1/2}(\sqrt{2}a)e^{S(x_2)}[e^{-\beta w_{10}(x_2)}j_k(LG(x_2)) - j_k(Lq(x_2))] \\ &\quad\times\int_{x_2}^\infty x_1^{3/2}K_{k+1/2}(\sqrt{2}a)e^{S(x_1)}[e^{-\beta w_{10}(x_1)}j_k(LG(x_1)) - j_k(Lq(x_1))]\,dx_1\,dx_2 \\ &\quad - \delta_{k,0}\int_0^\infty x_2^{3/2}I_{1/2}(\sqrt{2}a)e^{S(x_2)}[e^{-\beta w_{10}(x_2)} - 1]\int_{x_2}^\infty x_1^{3/2}K_{1/2}(\sqrt{2}a)e^{S(x_1)}[e^{-\beta w_{10}(x_1)} - 1]\,dx_1\,dx_2\ . \end{aligned} \tag{11}$$

I and K are modified Bessel functions of the first and third kind. j_k is a spherical Bessel function of order k. The asymptotic form for $P(\mathcal{E})$ developed in Ref. 7 is used to determine $P(\mathcal{E})$ for large values of $\mathcal{E}$.

B. Electron-broadening function $J(\omega,\mathcal{E})$

The interaction between the radiator and the electron perturbers is assumed to be a point-dipole interaction,

$$V_{\mathrm{int}} = e\vec{R}\cdot\vec{\mathcal{E}}_e(\vec{r})\ , \tag{12}$$

where $\vec{R}$ is the position operator for the bound radiator electron. $\vec{\mathcal{E}}_e(\vec{r})$ is the electric field at the position of the radiator due to an electron perturber located at $\vec{r}$. The matrix elements of R between bound hydrogenic states are proportional to Z^{-1}; thus the interaction V_{int} also scales as Z^{-1}.

In the case of the Lyman series, where there is no lower-state broadening, the relaxation theory expression for the quantity inside the square brackets of Eq. (2) becomes

$$[\Delta\omega - e\vec{\mathcal{E}}\cdot\vec{R}/\hbar - \mathcal{K}(\omega)]_{\mu\mu'} = \Delta\omega - e\mathcal{E}R^z_{\mu\mu'}/\hbar - \mathcal{K}(\omega)_{\mu\mu'}\ , \tag{13}$$

$$\mathcal{K}(\omega)_{\mu\mu'} = \hbar^{-2}\Gamma(\Delta\omega) \sum_{\mu''} \vec{R}_{\mu\mu''} \cdot \vec{R}_{\mu''\mu'} . \tag{14}$$

R^z is the z component of the position operator for the bound radiator electron. The atomic physics of the problem is explicit in the various matrix elements of R. The sum over μ'' runs over the quantum numbers of the upper level of the desired Lyman transition. In our case, Lyman α, μ'' runs over the quantum numbers of the $n=2$ excited state. It remains to determine $\Gamma(\Delta\omega)$, which contains the average electron-broadening effects.

In Ref. 8 the electron perturbers are treated as particles moving independently in the field of the charged radiator. The result for $\Gamma(\Delta\omega)$ is

$$\Gamma(\Delta\omega) = -i\left(\frac{4ne^4\lambda_T^3}{3\pi^2}\right) \int_0^\infty \int_0^\infty \int_0^\infty dk_1\, dk_2\, dt \exp\left[it\left(\Delta\omega + \frac{\hbar k_1^2}{2m} - \frac{\hbar k_2^2}{2m}\right)\right] \exp\left(-\frac{\hbar^2 k_1^2}{2m}\right) f(k_1, k_2) , \tag{15}$$

where n is the electron number density and λ_T is the electron thermal wavelength; $\vec{k}_1$ and $\vec{k}_2$ are wave vectors of the perturbing electrons;

$$f(k_1, k_2) = k_1 k_2 (\pi/2\sqrt{3}) g_{ff}(k_1, k_2) , \tag{16}$$

where g_{ff} is the free-free Gaunt factor discussed by Karzas and Latter[13] and by O'Brien.[14]

If we separate $\Gamma(\Delta\omega)$ into its real and imaginary parts, it can be shown that[8]

$$\Gamma_{\mathrm{Im}}(\Delta\omega > 0) = -\left(\frac{2ne^4}{3}\right)\left(\frac{8\pi m}{kT}\right)^{1/2}\left(\frac{2\pi}{\sqrt{3}\theta_R}\right) \times \int_0^\infty e^{-k_1^2/\theta_R} k_1 g(k_1, \chi_1)\, dk_1 , \tag{17}$$

$$\Gamma_{\mathrm{Im}}(\Delta\omega < 0) = e^{-|\Delta\omega|/\theta_R}\Gamma_{\mathrm{Im}}(\Delta\omega > 0) , \tag{18}$$

where $\chi_1^2 = k_1^2 + |\Delta\omega|$. Now, starting from the equation for $\Gamma(\Delta\omega)$, we can obtain a dispersion relation expressing $\Gamma_{\mathrm{Re}}(\Delta\omega)$ in terms of $\Gamma_{\mathrm{Im}}(\Delta\omega)$:

$$\Gamma_{\mathrm{Re}}(\Delta\omega) = \pi^{-1}\mathrm{P}\int_{-\infty}^{\infty} \frac{\Gamma_{\mathrm{Im}}(\omega')}{\omega' - \Delta\omega} d\omega' . \tag{19}$$

Hence we are able to use the computed values of $\Gamma_{\mathrm{Im}}(\Delta\omega)$ in evaluating the one-dimensional integral for $\Gamma_{\mathrm{Re}}(\Delta\omega)$. This procedure results in a large reduction in the necessary computer time compared to previous approaches.

In order to approximate the effect of electron correlations, we modify our ideal-gas result for $\Gamma_{\mathrm{Im}}(\Delta\omega)$ such that for $\Delta\omega < \omega_p$,

$$\Gamma_{\mathrm{Im}}(\Delta\omega < \omega_p) = \Gamma_{\mathrm{Im}}(\omega_p) . \tag{20}$$

This procedure is suggested by Fig. 1 of Ref. 15. If we impose the cutoff not at ω_p but at some fraction or multiple thereof, we find that the line center will be lowered or raised. However, the changes are small and quite insensitive to the variation in the cutoff frequency.

Once $\Gamma(\Delta\omega)$ has been computed, Eqs. (13) and (14) are employed in the computation of $J(\omega, \mathcal{E})$. In the case of Lyman α, the matrix inversion indicated in Eq. (2) may be performed analytically. The details of this matrix inversion and the trace over the states of the upper level of the transition are given in Ref. 16. The result is

$$J(\omega, \mathcal{E}) = C\,\mathrm{Im}\left\{\left[(\Delta\omega + 3A)\cosh\left(\frac{3a_0 e\mathcal{E}}{ZkT}\right) + \left(\frac{3a_0 e\mathcal{E}}{Z\hbar}\right)\sinh\left(\frac{3a_0 e\mathcal{E}}{ZkT}\right)\right] D^{-1} + \frac{2}{\Delta\omega + A}\right\} , \tag{21}$$

where

$$D = (\Delta\omega)^2 + 4\Delta\omega A + 3A^2 - (3a_0 e\mathcal{E}/Z\hbar) ,$$

and where C is a constant which is determined when the area under the line profile is normalized to unity. $A(\Delta\omega)$ is given by

$$A(\Delta\omega) = -(9a_0^2/Z^2\hbar^2)\Gamma_{\mathrm{Im}}(\Delta\omega) , \tag{22}$$

where a_0 is the Bohr radius. The nuclear charge of the radiator, Z, appears explicitly in Eqs. (21) and (22). It is also contained implicitly in $\Gamma(\Delta\omega)$, since the electron perturbers move in the Coulomb field of the hydrogenic radiator of charge $\chi = Z - 1$. That is, the charge of the radiator enters into the computation of the Gaunt factor.

At this point we briefly discuss the range of validity of the second-order theory that we have developed in this section. In dealing with high-temperature (10^6–10^7 °K) plasmas in the density range (1×10^{22})–(2×10^{23}) cm^{-3}, it might be expected that a second-order theory which is based on the assumption that the vast majority of collisions are weak and which does not include degeneracy effects would prove invalid. However, it can be shown that for the temperature-density conditions discussed in this paper, degeneracy effects are negligible.[17] To assess the relative strength of the electron interactions for the physical situations considered here, we first note that while the electronic attraction to an ionic radiator of charge $Z-1$ is proportional to $Z-1$, the binding energy of the bound radiator electron is proportional to Z^2. It follows that the ratio of the energy of such

an average electron-radiator interaction to the binding energy of the valence electron is approximately proportional to $n^{1/3}Z^{-1}$; for the worst case considered here, this ratio is approximately 1/10. Another indicator of relative electron-interaction strength that can be discussed is the ratio of the average electron-broadening effects to the average energy-level shift of the excited sublevels due to the static-electric-field interaction $e\vec{\mathcal{E}}\cdot\vec{R}/\hbar$ [see Eq. (13)]. This ratio is proportional to λ_T/r_0Z, where λ_T is the thermal wavelength for the electron. Again for cases described in this paper, this ratio will be less than 1/10. Hence even at the increased densities the assumptions inherent in a second-order theory are valid, at least in the first approximation.

Also, we expect that our theory will be valid inside the plasma frequency ω_p. Since $\omega_p = 2.72\times10^{-12}n^{1/2}$ (Rydberg units), we see that as the density increases the second-order theory becomes valid over a larger portion of the line profile.

III. RESULTS

A. Electric microfield distribution functions

In discussing our results we will rely on Figs. 1–3.

Figures 1 and 2 illustrate how the probability distribution function for finding a given electric field at multiply charged radiators, immersed in a "gas" of singly-charged ions, changes as a function of the parameter a. Figure 3 shows a comparison of the distribution functions for three different values of radiator charge χ at a given value of a.

From these figures and graphs we observe that the effect on the distribution function when χ is made greater than unity is similar to that which occurs, for $\chi=1$, when a is increased (T is decreased and/or n is increased). That is, as shown in Fig. 3, for $\chi>1$, the peak of the distribution is shifted to smaller values of $\mathcal{E}$, becomes narrower, and has its maximum value increased.

Furthermore, a comparison of Figs. 1 and 2 with Fig. 4 of Ref. 7 reveals that as χ increases the relative sensitivity to changes in a increases. This increased sensitivity is due to the fact that in many functions written in Sec. II A the parameter a^2 is multiplied by χ.

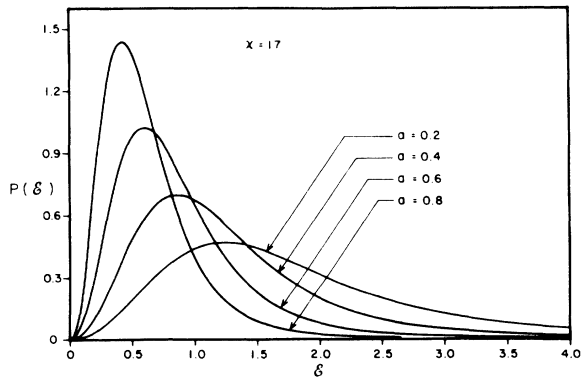

FIG. 1. Electric microfield distribution function $P(\mathcal{E})$ at a point having a charge of +17. $\mathcal{E}$ is in units of $\mathcal{E}_0$ $(=e/r_0^2)$ and $a=r_0/\lambda_D$. Tables corresponding to these curves are available upon request.

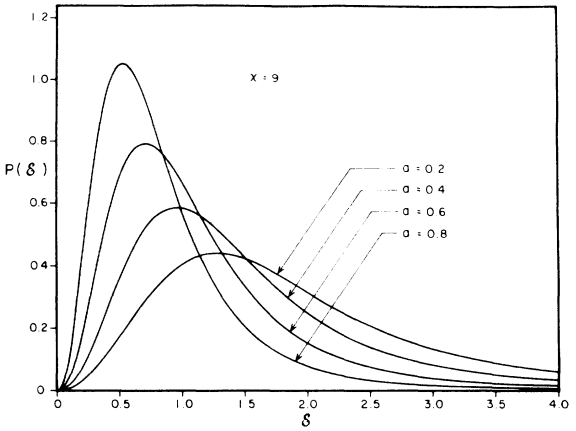

FIG. 2. Same as Fig. 1, but at a point having a charge of +9. Tables corresponding to these curves are available upon request.

B. Line profiles

Figure 4 shows the relative contributions to the Lyman-α Ne X line profile from the several broadening mechanisms that are included in our calculations, together with the combined result. The conditions represented in Fig. 4 correspond to an

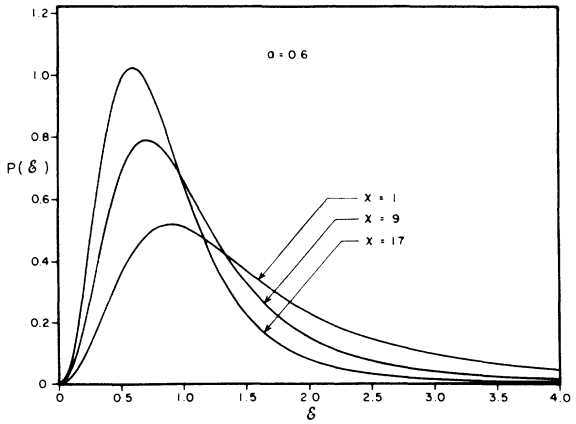

FIG. 3. Electric microfield distribution functions $P(\mathcal{E})$, for $a=0.6$, at points corresponding to $\chi=1$, 9, and 17.

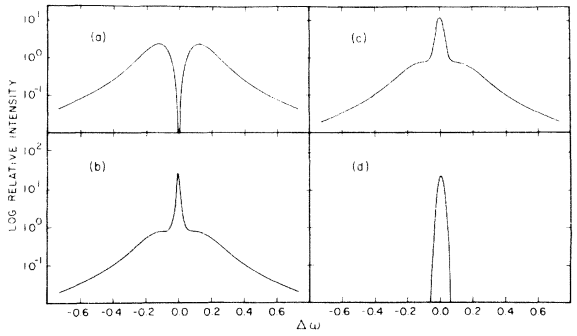

FIG. 4. Line profiles for the Lyman-α line of Ne X, illustrating various contribution to the complete line profile: (a) static-ion profile, (b) profile including static ions and dynamic electrons, (c) profile including static ions, dynamic electrons, and the Doppler effect, (d) Doppler profile. $T = 809.1$ eV and $n = 1\times10^{23}$ cm^{-3}. $\Delta\omega$ is in rydbergs.

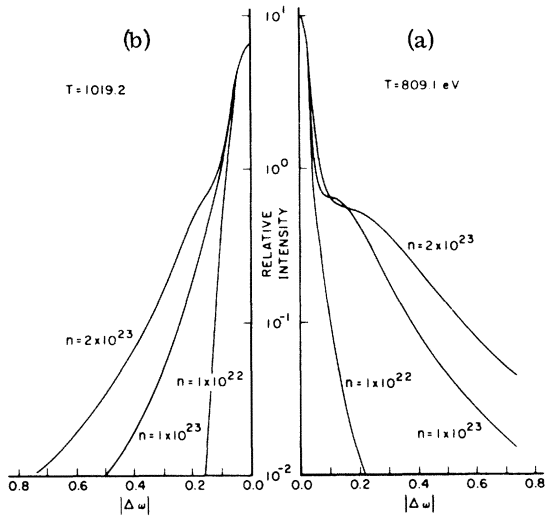

FIG. 6. (a) Ne X and (b) Ar XVIII Lyman-α line profiles, each of which corresponds to the same temperature but different density. $\Delta\omega$ is in rydbergs.

a value of 0.4. The relative importance of the Doppler effect is of interest. For the temperatures discussed in this paper, the Doppler effect is much more significant—compared to the electron-broadening contribution—than was the case when dealing with more conventional plasmas (e.g., $n = 10^{17}$ cm^{-3} and $T = 40\,000\,^{\circ}$K). The qualitative features of the Stark profile are also different: here the electron contribution produces a sharp spike which sits on shoulders provided largely by the ions. Figure 5 presents a plot for Ar XVIII that is equivalent to Fig. 4 for Ne X. The qualitative information is the same.

Figure 6 shows, for both Ne X and Ar XVIII, families of profiles, each of which corresponds to the same T but different n. It is evident that as n increases, the profile changes greatly, both in shape and width, thereby illustrating the density sensitivity of the line profile. The practical sensitivity that might be inferred from comparison of experimental and theoretical line shapes depends on at least two factors, (1) How much of the line profile can be experimentally observed, and (2) the resolution of the x-ray spectrometer used.

Figure 7 shows for Ne X and Ar XVIII, families of three curves, each of which corresponds to the same density but different T. The results here imply that the frequently mentioned insensitivity of plasma-broadened line profiles to variations in T is significantly reduced as χ increases. The fact that Doppler broadening plays a more significant role in broadening the argon lines than it does for neon is due to the fact that the effect depends not only on mass, but also on the radiator Z.

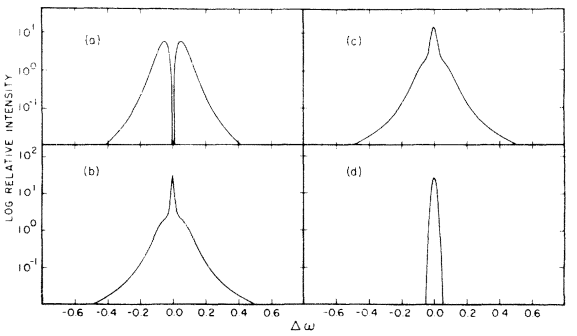

FIG. 5. Same as Fig. 4, but for Ar XVIII; $T = 113.2$ eV and $n = 2\times10^{23}$ cm^{-3}.

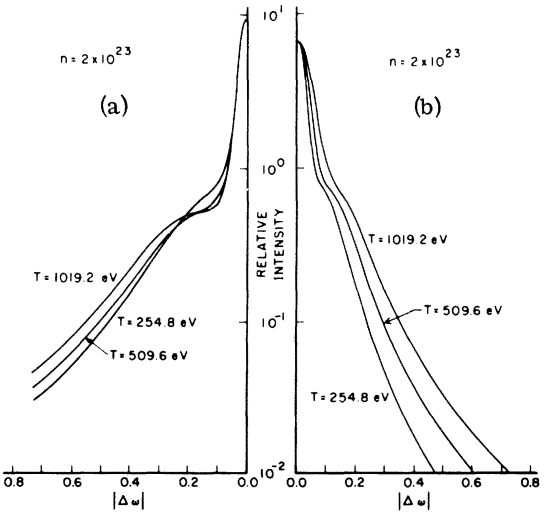

FIG. 7. Same as Fig. 6, but for the same density with different temperature.

IV. SUMMARY

The results illustrated and discussed in this paper suggest that the diagnostic potential of plasma-line-broadening which has been clearly demonstrated when applied to conventional plasmas[10,18] will carry over to laser-produced plasmas where the emitted lines are in the x-ray region. However, the decreased temperature insensitivity implies that the use of several series members should be used to better determine the density and also to provide a consistency check on other temperature determinations.

Our deliberations have thus far been based on rather ideal assumptions: optical thinness and fixed temperature and density. We are in the process of extending our calculations to higher series members, where the effects of optical thickness will be reduced. Secondly, we are modifying our theory to allow for different ion and electron kinetic temperatures. Finally, we expect to produce time-averaged profiles, so that we may more realistically analyze experimental data. Toward this end, it should be mentioned that the line profiles illustrated here were very inexpensive to produce—approximately $\frac{1}{20}$ the cost of those illustrated in Ref. 8.

We are also in the process of extending our electric microfield and line-profile calculation to cases where the radiator has charge $Z-1$ and the perturbers are hydrogenic $(Z-1)$ and heliumlike $(Z-2)$ ions in varying ratios.

ACKNOWLEDGMENTS

We would like to thank Dr. George F. Chapline of the Lawrence Livermore Laboratory for suggesting this research and Dr. Hugh E. DeWitt (also of LLL) and Dr. Robert L. Coldwell (Univ. of Florida) for several helpful discussions.

---

*Work supported in part by the Lawrence Livermore Laboratory and by the Northeast Regional Data Center of the State University System of Florida.

[1]A. V. Vinogradov, I. I. Sobel'man, and E. A. Yukov, Kvant. Elektron. (Mosk.) 1, 268 (1974) [Sov. J. Quant. Electron. 4, 149 (1974)].

[2]F. E. Irons, J. Phys. B 6, 1562 (1973).

[3]V. A. Batanov, V. A. Bogatyrev, N. K. Sukhodrev, and V. B. Fedorov, Zh. Eksp. Teor. Fiz. 64, 825 (1973) [Sov. Phys.-JETP 37, 419 (1973)].

[4]B. Yaakobi and L. M. Goldman, Bull. Am. Phys. Soc. 20, 1302 (1975).

[5]P. G. Burkhalter, Bull. Am. Phys. Soc. 20, 1302 (1975).

[6]George F. Chapline, Hugh E. DeWitt, and C. F. Hooper, Jr., UCRL Report No. 76272, 1974 (unpublished).

[7]John T. O'Brien and C. F. Hooper, Jr., Phys. Rev. A 5, 867 (1972).

[8]John T. O'Brien and C. F. Hooper, Jr., J. Quant. Spectrosc. Radiat. Transfer 14, 479 (1974).

[9]E. W. Smith and C. F. Hooper, Jr., Phys. Rev. 157, 126 (1967).

[10]H. R. Griem, *Spectral Line Broadening by Plasmas* (Academic, New York, 1974).

[11]C. F. Hooper, Jr., Phys. Rev. 165, 215 (1968).

[12]C. F. Hooper, Jr., Phys. Rev. 149, 77 (1966).

[13]W. J. Karzas and R. Latter, Astrophys. J. Supp. 55, 167 (1961).

[14]John T. O'Brien, Astrophys. J., 170, 613 (1971).

[15]E. W. Smith, Phys. Rev. 166, 102 (1968).

[16]John T. O'Brien, Ph.D. thesis (Univ. of Florida, 1970) (unpublished).

[17]Hugh E. DeWitt, *Low-Luminosity Stars* (Gordon and Breach, New York, 1969), Paper III-2.

[18]H. R. Griem, *Plasma Spectroscopy* (McGraw-Hill, New York, 1964).